THEORETICAL AND EXPERIMENTAL STUDY OF THE JOSEPHSON EFFECT IN SUBMICRON *SN-N-NS* STRUCTURES

Yu. P. Baryshev, A.G. Vasil'ev, A.A. Dmitriyev, M. Yu. Kupriyanov, V.F. Lukichev, I. Yu. Luk'yanova, A.A. Orlikovskiy and I.S. Sokolova

Introduction

It was long thought that an *SNS*-type variable-thickness microbridge was the most promising structure for various applications of the Josephson effect. The first theoretical estimates [1-3] of the possible parameter values of these structures showed that variable-thickness microbridges should have high values of characteristic voltage $V_c=I_cR_N$ (I_c is the critical current of the junction; R_N is the resistance of the junction in the normal state) and significantly lower capacitance than in tunnel junctions. However, attempts to implement variable-thickness microbridges with satisfactory characteristics encountered both technological and theoretical difficulties. The former were related to the need to control the reproduction of the small gaps (on the order of 0.1 μm) between superconducting electrodes, while the latter were related to the lack of well-founded criteria for selection of the optimal *S*- and *N*-material pairs to form the junction. This situation gave the advantage to tunnel technology development.

The latest achievements in microelectronics, allowing reproduction of lines on the order of 10 nm in width, permit the manufacture of variable-thickness microbridges. This brings up the need for the most complete possible understanding of processes occurring in these structures. In recent times, works

have appeared [4-6] describing experimental Josephson variable-thickness microbridges with weak coupling area dimensions of less than 0.1 μm. However, the results of these works served primarily as a demonstration of the capabilities of submicron technology, while the question of the criteria for selection of materials for electrodes and bridge jumpers yielding high values of the parameter V_c remained open.

The results of the first experiments with variable-thickness microbridges differed significantly from the theoretical estimates [1-3] which, in our opinion, can be explained by the following factors: The unjustifiably "rigid" boundary conditions[1], the use of which resulted in excessive estimates of V_c for actual structures and failure to consider the possible influence of effective electron repulsion in the bridge jumper material. We shall show below that the question of boundary conditions is directly related to the problem of selecting electrode and bridge jumper materials. We shall not consider variable-thickness microbridges of a single material due to the unacceptably high requirements thus placed on minimum weak coupling dimensions, nor vertical-type bridges, rarely manufactured by group integrated circuit technology.

In what follows we shall theoretically justify criteria for selecting materials for *SN–N–NS* structures, describe manufacturing technologies on the example of Nb-Al-Nb variable-thickness bridges, present their characteristics and an experimental confirmation of the correctness of the criteria found for selecting materials, and determine areas for future research.

1. Model of *SN–N–NS* Microbridge and Its Description

Figure 1 shows the geometry of the *SN–N–NS* microbridge, in which the superconducting *S* layer contacts the *N*–metal film over its entire surface, so that the microbridge electrode is an *SN* sandwich. It is assumed that the "dirty" limiting conditions are met in the *S–N*–metal junction, there are no potential barriers at the boundaries, and the critical *N*–metal temperature T_{cN} is equal to zero. In performing specific calculations, we ignored suppression of electrode superconductivity both by the current flowing through and by the reverse influence of the microbridge jumper on the status of the compound *SN* electrodes. These superconducting electrodes are considered massive, i.e., with thickness d_S exceeding the length of coherence of the superconductor $\xi(T)$:

$$d_S > \xi(T) = (\pi/2)\xi_S^*(1-T/T_c)^{-1/2}, \qquad \xi_S^* = (D_S/2\pi T_c)^{1/2}, \qquad (1)$$

while the thickness of the normal film is rather small:

[1]Having in mind conditions on the Green functions F_ω at the *SN* boundary, requiring that F_ω be equal to their equilibrium values in the superconductor, which is correct if the superconducting electrodes remain in the unexcited state.

$$d_N<\min\{\xi_S^*, \xi_N^*\}, \qquad \xi_N^*=(D_N/2\pi T_c)^{1/2}. \tag{2}$$

Here D_S and D_N are the diffusion coefficients of electrons in the S and N metals. Suppose, furthermore, that quasihomogeneity conditions are met in the microbridge film, i.e., width w is limited as follows

$$w<\lambda_J, \tag{3}$$

where λ_J is the Josephson penetration depth. When all of these conditions are met, the problem of investigating the steady-state properties of $SN-N-NS$ microbridges is reduced to successive solution of two homogeneous problems within the framework of the equations of Usadel.

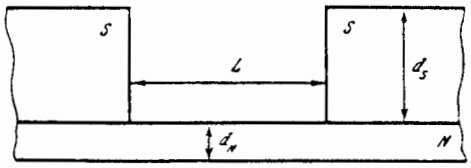

Figure 1. Schematic Image of $SN-N-NS$ Variable Thickness Microbridge Structure.

The first problem is to study the proximity effect in a compound SN electrode and find the values of the Green function F_ω at the SN interface. The second problem is to compute the critical transition current based on the values of F_ω found in the first problem at the SN boundary. These values will be less than in a homogeneous superconductor, since the proximity effect in the SN electrode partially suppresses the superconductivity of the S layer which, in turn, decreases the values of V_c in comparison to the case with no suppression.

The degree of this suppression, as was shown in our earlier work [7], depends on the properties of the S and N metals and is determined by the parameter

$$\gamma_M=\gamma d_N/\xi_N^*, \qquad \gamma=\sigma_N\xi_S^*/\sigma_S\xi_N^* \tag{4}$$

where $\sigma_{N,S}$ represents the conductivity of the N and S metals in the normal state. This same work also studies the variation in characteristic voltage V_c as a function of parameter γ_M.

With no suppression of superconductivity in the electrodes (γ_M=0, rigid boundary conditions) at the limit of maximum junction lengths $L \gg \xi_N = (D_N/2\pi T)^{1/2}$, the critical current is determined by the equation [8]

$$I_c = I_0 = \frac{64\,\pi T}{eR_N} \frac{\Delta_\infty^2 L/\xi_N \exp(-L/\xi_N)}{[\pi T + \Delta^* + \sqrt{2}\,[\Delta^*(\Delta^* + \pi T)]^{1/2}]^2}, \qquad (5)$$
$$\Delta^* = [(\pi T)^2 + \Delta_\infty^2]^{1/2},$$

which yields a linear variation of $I_c \sim (1 - T/T_c)$ near the critical temperature, Δ_∞ is the equilibrium value of the order parameter in the S layer.

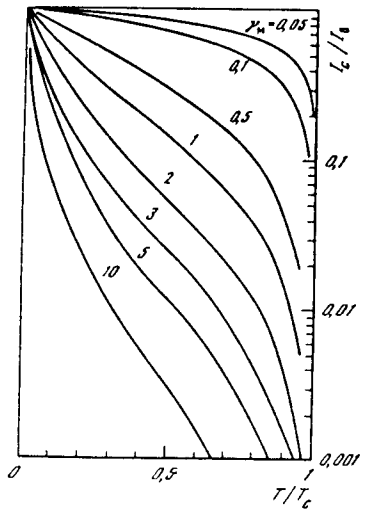

Figure 2. Ratio of Critical Current I_c of SN–N–NS Microbridge to Its Value I_0 Where γ_M=0 (cf. (5)) as a Function of Temperature and Parameter γ_M.

As the parameter γ_M increases, the critical current is suppressed. Figure 2 shows the temperature variation of I_c/I_0 for various values of γ_M [7]. As we can see from this figure, this suppression is greater, the closer T is to T_c. Thus, for $\gamma_M \approx 1$ in the area of moderate temperature ($T \approx T_c/2$) the critical current is less than the limiting current (cf. (5)) by an order of magnitude, while where $T \approx 0.9\,T_c$ it is less by two orders of magnitude.

In the case of finite junction lengths, as in the case of great lengths, a decrease in I_c with fixed γ_M is manifested most strongly in the area of $T \approx T_c$. However, at relatively small γ_M and $L \ll \xi_N^*$, the suppression of critical current due to the proximity effect in the electrodes occurs more uniformly throughout the entire temperature interval. In the most interesting length area $L \lesssim 3\xi_N^*$ at temperatures which are not too high $T \approx T_c/2$, the critical current even at $\gamma_M \approx 0.3$ is approximately half the value calculated in [3] for $\gamma_M = 0$.

Thus, the theory which has been developed allows us to drawn an important conclusion: Rigid boundary conditions and, consequently, maximum values of V_c are achieved in *SN–N–NS*-type microbridges at small values of the parameter γ_M:

$$\gamma_M \lesssim 0.3. \qquad (6)$$

The results obtained are correct where $T_{cN} = 0$, i.e., the effective electron-phonon interaction content of the electrons λ_N in the weakly coupled material is also equal to zero. Clearly, the difference of λ_N from zero can influence the critical current, decreasing it where $\lambda_N < 0$ (effective repulsion of electrons). In [9] within the framework of rigid boundary conditions (correct, as we have shown, where $\gamma_M < 0.3$) it was established that effective electron repulsion slightly decreases the critical junction current in comparison to the case where $\lambda_N = 0$. A convenient parameter describing the force of repulsion is a quantity with the dimension of temperature

$$T^* = 1.14\omega_D \exp\{-1/\lambda_N N_N(0)\} \gg \omega_D, \ \lambda_N < 0, \quad k_B = \hbar = 1, \qquad (7)$$

where ω_D is the Debye frequency; $N_N(0)$ is the density of states on the Fermi surface of the N metal.

Calculations of the function $V_c(T)$ performed for various T_c/T^* have shown that effective repulsion of electrons appears most strongly in the low temperature area $T \lesssim T_c/2$; the characteristic voltage V_c decreases in comparison with a "true normal" metal ($\lambda_N = 0$) by only 20% with rather strong repulsion $T_c/T^* = 10^{-3}$. For example, in actual ratios $T_c/\omega_D \approx 0.03$, the value of $T_c/T^* = 10^{-3}$ corresponds to $|\lambda_N| \approx 0.3$, which would yield $T_{cN}/T_c = 0.9$ if electrons were attracted with that force.

Thus, the influence of effective electron repulsion is slight in comparison to the influence of the proximity effect in electrodes on the steady properties of *SN–N–NS* junctions. This means that to achieve the minimum value of V_c it is most important to decrease the influence of the proximity effect in electrodes by selecting materials for the microbridge jumper and electrodes assuring that parameter γ_M is small.

2. Optimization of Variable Thickness *SN–N–NS* Microbridge Parameters

The most important characteristics of Josephson junctions are the characteristic voltage $V_c=I_cR_N$ and resistance in the normal state R_N. Let us determine the values of parameters and microbridge geometry for which V_c is maximal, while resistance R_N is not too small. We note that the optimal values of the parameters depend on the optimization criteria selected.

Since the basic mechanism for suppression of V_c is the proximity effect in the electrodes, as the first criterion we demand that this effect be small, for example considering the effect small if V_c decreases by a factor of not more than 2. This criterion is reasonable, since, as will be shown below, it approaches values of $V_c \geqslant 1$ mV as a result of optimization, which is desirable for most applications. This criterion, as we shall show below, is met with condition (6).

All of the theoretical analysis above was performed on the assumption that: 1) There is no suppression of the superconductivity of the electrodes by the current; 2) the inverse influence of the proximity effect between the jumper and *SN* electrode is small; 3) the junction is concentrated. As was shown in [10], these three conditions place additional limitations on the parameter γ_M. The first two limitations are as follows

$$\gamma_M \leqslant \begin{cases} L/\xi_N^* \max\{L/\xi_N^*, \xi_S^*/\xi_N^*\}, & \text{where } L \ll \xi_N^*, \\ \exp(L/\xi_N^*) \max\{\xi_S^*/\xi_N^*, \exp(L/\xi_N)\}, & \text{where } L \gg \xi_N, \end{cases} \tag{8}$$

$$\gamma_M \leqslant 0{,}5 \max\{1, \xi_N^*/L\} \max\{1, \xi_S^*/\xi_N^*\}. \tag{9}$$

The next condition (concentrated junction) depends essentially on whether the junction is located above a superconducting shield:

$$\text{above shield } \gamma_M \leqslant \frac{\lambda_S}{w}\frac{\lambda_S}{t_e}\frac{\xi_S^*}{\xi_N^*} \begin{cases} L/\xi_N^*, & \text{where } L \ll \xi_N^* \\ \exp(L/\xi_N), & \text{where } L \gg \xi_N, \end{cases} \tag{10a}$$

$$\text{without shield } \gamma_M \leqslant \frac{\lambda_S^2}{w^2}\frac{\xi_S^*}{\xi_N^*} \begin{cases} L/\xi_N^*, & \text{where } L \ll \xi_N^* \\ \exp\{L/\xi_N\}, & \text{where } L \gg \xi_N, \end{cases} \tag{10b}$$

where λ_S is the depth of penetration of the magnetic field into the superconductor; t_e is the effective distance from the shield.

Value of Parameter $\gamma=\sigma_N\xi_S^*/\sigma_S\xi_N^*$ for Various S- and N- Materials

N \ S	Pb($\rho_{300}/\rho_{10}\approx10$) ($\lambda_S\approx30$ nm, $\xi_S^*\approx93$nm, $\sigma_S^{-1}\approx10^{-8}$ Ohms·m)	Nb($\rho_{300}/\rho_{10}\approx3$) ($\lambda_S\approx32$ nm, $\xi_S^*\approx40$ nm, $\sigma_S^{-1}\approx2\cdot10^{-8}$ Ohms·m)	Nb_3Sn ($\lambda_S\approx170$ nm, $\xi_S^*\approx4$ nm, $\sigma_S^{-1}\approx1.5\cdot10^{-6}$ Ohms·m)	NbN ($\lambda_S\approx600$ nm, $\xi_S^*\approx4$ nm, $\sigma_S^{-1}\approx3\cdot10^{-6}$ Ohms·m)
Mono-Si* ($n^*\approx10^{20}$ cm^{-3}, $\xi_N^*\approx15$ nm, $\sigma_N^{-1}\approx2\cdot10^{-5}$ Ohms·m)	$3\cdot10^{-3}$	$3\cdot10^{-3}$	$2\cdot10^{-2}$	$4\cdot10^{-2}$
Poly-Si* ($n^*\approx10^{20}$ cm^{-3}, $\xi_N^*\approx3$ nm, $\sigma_N^{-1}\approx10^{-5}$ Ohms·m)	$3\cdot10^{-2}$	$3\cdot10^{-2}$	0.2	0.4
n-InAs ($n^*\approx2.6\cdot10^{18}$ cm^{-3}, $\xi_N^*\approx60$ nm, $\sigma_N^{-1}\approx3\cdot10^{-6}$ Ohms·m [11])	$5\cdot10^{-3}$	$4\cdot10^{-3}$	$3\cdot10^{-2}$	$7\cdot10^{-2}$

Let us analyze the case of a microbridge over a superconducting shield and show the area assigned by equations (6), (8)-(10) in the plane (γ_M, L) (Figure 3, shaded). Since V_c decreases exponentially with increasing L, we must select $L\lesssim\xi_N^*$. However, decreasing L for concentrated junctions results in strong limitations on γ_M and, furthermore, a decrease in the resistance $R_N(R_N\sim L)$. The optimal length from the standpoint of these contradictory requirements is length $L\approx\xi_N^*$, for which parameter γ_M should be quite small:

$$\gamma_M\lesssim\lambda_S^2\xi_S^*/wt_e\xi_N^* \qquad (11)$$

Let us now estimate the parameters for certain widely used materials. The table presents estimated values of the parameter $\gamma=\sigma_N\xi_S^*/\sigma_S\xi_N^*$ for the ma-

terials studied earlier (cf. references in [10]). Let us estimate, for one of the best studied pairs of materials Nb–InAs [11], the parameters of microbridges above a superconducting shield.

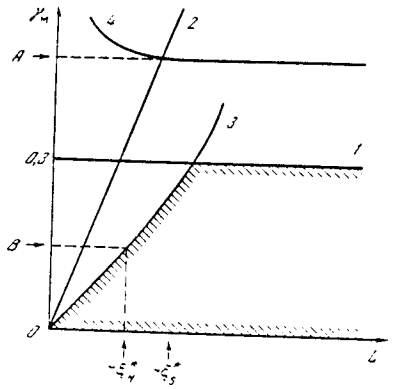

Figure 3. Diagram of Variable-Thickness Microbridge Parameter Areas in the Plane (γ_M, L) Within Which the Proximity Effect Can Be Ignored in Electrodes (6) (Line *1*); Suppression of Electrode Superconductivity by Current (8) (Line *2*); Phase Difference Across Microbridge Width (10) (Curve *3*); Proximity Effect Between Jumper and Compound *SN* Electron (9) (Curve *4*) ($A \sim 0.5\ \xi_S^*/\xi_N^*$, $B \sim \lambda_S^2 \xi_S^*/wt_e\xi_N^*$). Shaded area corresponds to concentrated junctions with maximum possible value of I_cR_N.

According to conditions (11) for typical values of $w \approx 2$ μm, $t_e \approx 0.3$ μm for an Nb–InAs–Nb bridge we obtain the limit of γ

$$\gamma \lesssim \frac{\lambda_S^2 \xi_S^*}{wt_e \xi_N^*} \frac{\xi_N^*}{d_N} \approx 10^{-3} \frac{\xi_N^*}{d_N}, \tag{12}$$

from which we obtain the limit of the maximum N-layer thickness

$$d_N \lesssim (d_N)_{\max} \approx 0.3\ \xi_N^* \approx 20 \text{ nm}. \tag{13}$$

The normal-state resistance of this microbridge is on the order of $R_N \approx 10$ Ohms. The last limitation may be somewhat weakened due to the reduced bridge width w.

The estimates presented show that to produce variable-thickness microbridges of widely used materials with high characteristic voltage V_c(≥1 mV) we must create very thin (~20–40nm) normally conductive high-resistance layers with good carrier mobility. Creation of such layers by deposition or ion implantation of impurities in a semiconductor surface lies practically at limits of the capabilities of these methods. Thus, we must search for new ways to create such layers with small values of γ_M. High-quality single-crystal n-type layers with high electron mobility on the semiconductor surface, produced by molecular-beam epitaxy and other methods are promising materials from this standpoint. However, investigation of the suitability of any pair of S and N materials as materials for Josephson junctions requires a direct method for measuring the parameter γ_M without measuring the quantities which define it, before the actual junction is created. Methods of measuring parameter γ_M are described in the Appendix.

3. Experimental Work

The technology developed for manufacturing SN–N–NS microbridges can be divided into two independent steps: Formation of the type N microbridge

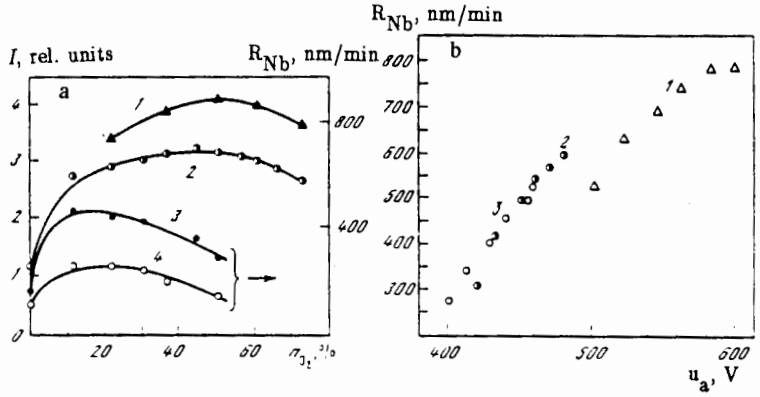

Figure 4. Emissions of CO_2^+(288 nm) and F (703.7 nm) and Etching Rate of Nb as a Function of O_2 Content (a), as well as Variation in Etching Rate of Nb as a Function of Amplitude of Potential Space Charge Area (b). a: 1 — CO_2^+; 2 — F; 3 and 4 — flow rate of CF_4-O_2 100 and 25 cm^3/min; b: 1 — pressure in chamber 20 Pa; 2 — 51 Pa; 3 — 70 Pa.

jumper and formation of the superconducting electrodes. The jumper can be formed by several methods, one of which is to apply and structure a film of a normally conductive metal. Aluminum was suggested as the model jumper material. A film of Al 50-60 nm thick was applied to an Si substrate with orientation (111) heated to t=200-230°C by electron-beam evaporation under "industrial" vacuum ($7 \cdot 10^{-5}$ Pa) at 0.2 nm/s. Lift-off electron lithography was used to form the jumpers of Al up to 1 μm wide. Although microbridges with Al jumpers are not optimal from the standpoint of high values of V_c, their investigation can be used to test the basic conclusions of the theory developed above.

The second stage is the creation of superconducting electrodes. Niobium was used as the electrode material, since it had high critical temperature and good mechanical properties.

High quality Nb films were produced using the method of condensation with autoion bombardment under an "industrial" vacuum [12], as well as electron-beam evaporation under high vacuum (10^{-7} - 10^{-8} Pa) with preliminary cleansing of the Si surface with Ar^+ ions with energy 0.5-0.7 keV. Both methods can produce superthin (less than 200 nm) Nb films with low content of interstitial gas impurities. In the former method with intensive ion bombardment the substrate is a significant source of (O, C) impurities. Therefore, preference was given to films produced under high-vacuum conditions. Films 200 nm thick had T_c=9.0 K and R_{300}/R_{10}=6.

The most preferable method of microstructuring Nb films is plasma etching, since in contrast to the ion and ion-chemical methods this process does not result in significant deterioration of the superconducting properties of Nb films and structure of Al films.

To determine the influence of plasma process parameters on the rate and anisotropy of etching, etching of Nb in a CF_4-O_2 plasma through an electron-resist mass was studied [13]. The selection of gases was determined by the high selectivity of etching of Nb in CF_4 with respect to Al.

The plasma etching process was studied in a diode-type reactor with plane-parallel electrodes. The specimen was placed on the lower, grounded electrode. The specimen temperature was set to 20°C and maintained with an error of ±1°C. The pressure in the chamber was varied between 33 and 133 Pa, the generator power at 75-200 W, oxygen content in the mixture 0-80%. The generator frequency was set at 75 kHz. During etching, the emission spectra of the plasma was measured in the 200-800 nm wavelength band, peak values of voltage at the anode (V_p) and gas flow were monitored.

The moment of completion of etching was determined by the change in the intensity of CO_2^+ and F emissions. Figure 4*a* shows the Nb etching rate and

CO_2^+ and F emission intensities as functions of oxygen content in the CF_4-O_2 gas mixture. The concentration of atomic fluorine n_F in the plasma was estimated using Ar calibration by optical spectroscopy, indicating an almost linear variation of n_F with pressure in the 10-10^2 Pa range.

Figure 5. Photomicrograph of Nb-Al-Nb Microbridge of Variable Thickness.

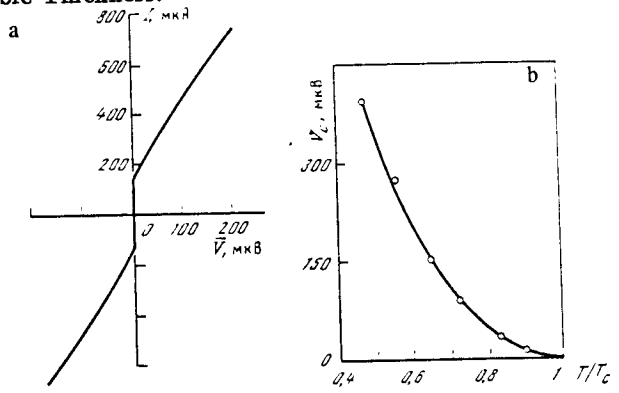

Figure 6. Volt-Ampere Characteristics of Nb-Al-Nb Variable Thickness Microbridge (a) and Temperature Variation of Characteristic Voltage V_c for Nb-Al-Nb Microbridge (b) (T_c=9 K, R_N≈0.4 Ohms). Solid curve shows theoretical function $V_c(T)$ for γ_M=1.0 and $L \ll \xi_N^*$

The variation in etching rate as a function of pressure in the chamber was characteristic for plasma etching of Nb. As pressure dropped to 20 Pa, a great increase was observed in rate (up to 800 nm/min) and anisotropy of etching which, in our opinion, is explained by the increased significance of ion bombardment (for example, CF_3^+ [13]) of the Nb surface. This is confirmed by the increase in maximum voltage at the anode (to 600 V — cf. Figure 4*b*) and, consequently, the energy of ions accelerated in the cathode area of the space charge, as well as the sharp decrease in etching rate of the Nb covered by the perforated metal screen, which captured charged particles.

The experiments described above were used to find conditions allowing selective anisotropic etching of Nb films through an electroresist mask and create a structure in the Nb with minimum slot size 0.25 μm.

A photomicrograph of an Nb–Al–Nb junction made by double electron-beam lithography and plasma etching with $d_N \approx 0.05$ μm, $d_S \approx 0.2$ μm, $w=1$ μm and $L=0.25$ μm is shown in Figure 5.

Typical values of R_N of the junctions achieved were 0.1–0.8 Ohms. Figure 6*a* shows the volt-ampere characteristic of a junction at $T=5.5$ K. The value of V_c is about 50 μV. This very low value of V_c results from the strong proximity effect in the electrodes, since aluminum is a better conductor than is niobium ($\sigma_S \approx 0.1\ \sigma_N$ in this case). For this reason, we should expect relatively large values of γ_M. The methods of experimental measurement of this parameter are discussed in detail below and require additional research, not undertaken in the present work. However, even the available curves of $V_c(T)$ (Figure 6*b*) can be used to estimate γ_M in terms of its order of magnitude. Considering $L \ll \xi_N^*$ and $\Delta_0/e \approx 1$ mV for Nb, a comparison with the theoretical curve for $L \ll \xi_N^*$ yields an estimate for the coherence length in Al of $\xi_N^* \approx 0.1$ μm, which agrees in order of magnitude with the quantity $\xi_N^* \approx (\xi_0 d_N)^{1/2} \approx 0.3$ μm, where $\xi_0 = 1.6$ μm is the theoretical length of coherence in pure, massive aluminum [14].

Conclusions

The studies performed in this work allow us to draw the important conclusion that at the current stage of development of microelectronics, *SN–N–NS* Josephson variable-thickness microbridges are promising structures for various Josephson-effect applications. To create junctions with the optimal parameters, we must select a pair of *S* and *N* materials providing small values of the parameter γ_M. Estimates made for widely used materials have shown that search for

and study of new materials for microbridge jumpers are needed. These studies using *SN, SNIN* and *NSIN* test structures need not involve manufacture of a junction itself. One advantage of the methods suggested for determining parameter γ_M is the possibility of considering the influence of the most important technological factors, which would be difficult to consider by measuring the quantities determining them directly. Narrow-zone degenerate semiconductors with high charge-carrier mobility, as well as refractory metal silicides, can be considered promising materials.

The criteria for optimization of Josephson-junction parameters selected in this work are correct for most applications, particularly for computer applications. However, there are certain areas of use of the junctions, for example as stress standards, for which certain absolute values of characteristic voltage V_c are required. Thus, to produce the maximum of the first current step on the voltage-ampere characteristic when the junction is exposed to microwave radiation, ideally the microwave frequency and characteristic frequency of the Josephson junction $\omega_c=2eV_c/\hbar$ should be approximately equal. In the three-centimeter waveband this condition corresponds to $V_c\approx 20$ μV, which is about similar in order of magnitude to the values obtained in this work for Nb-Al-Nb microbridges.

We studied quasiunidimensional planar-type structures. The influence of quasi-two-dimensionality on the basic properties of the junctions, as was shown in [15], introduces no significant peculiarities in comparison to the quasiunidimensional case. In particular, in spite of the fact that the critical current I_c as a function of d_N has a maximum at $d_N\approx\xi_N^*$, the parameter $V_c\approx I_cR_N$ decreases monotonically with increasing d_N and does not exceed the value for quasiunidimensional junctions, as was erroneously affirmed in [16].

In conclusion, the authors expressed their gratitude to academician K. A. Valiyev for his constant attention to their work, to A. D. Krivospitskiy for assistance in manufacturing the junctions, and to L. S. Kuzmin for his assistance in performing measurements.

Appendix

Methods of Measuring the Parameter γ_M

***SN* sandwich critical temperature measurement.** We know that the proximity effect causes the critical temperature T_c^* of an *SN* sandwich to depend on *S*-layer thickness. At the limit $d_S\to 0$, T_c^* approaches zero, while for a thicker superconductor layer ($d_S\gg\xi_S^*$) the value of T_c^* approaches its value in a massive

superconductor. The function $T_c^*(d_s)$ was computed in (17) for various values of γ_M, as shown in Figure 7*a*. A comparison of the experimental curves of $T_c^*(d_S)$ for the pair of *S* and *N* materials studied with the theoretical values allows us to estimate the parameter γ_M. To do this, we must know ξ_S^*, which can be easily found from measurements of the critical magnetic field H_{c2} near the critical temperature.

Measurement of critical *SN*-sandwich magnetic field. Suppression of the order of parameter in the *S* layer of the sandwich leads to a change in critical magnetic field H_{c2}, which is a function of thickness d_S and parameter γ_M. As was shown in [18], the value of this field is determined by the following expressions:

$$H_{c2}(T, d_S) = H_S \frac{4}{\pi^2}(1 - T/T_c) - H_p, \quad H_p = \frac{\Phi_0}{2\pi\xi_S^{*2}} = \frac{\pi^2}{4} T_c \left| \frac{dH_{c2}}{dT} \right|_{T=T_c}, \quad (14)$$

$$\sqrt{\frac{H_p}{H_s}} \operatorname{tg}\left(\frac{d_S}{\xi_S^*}\sqrt{\frac{H_p}{H_s}}\right) = \gamma_M \left(1{,}17 + \frac{2}{\pi^2}\ln(1 + 0{,}98\,\gamma_M^{-2})\right), \quad (15)$$

where Φ_0 is the magnetic flux quantum. Assuming formally $T=0$ in (14), we obtain

$$H_p = \frac{1}{T_c}\left| \frac{dH_{c2}}{dT} \right|_{T=T_c} - H_{c2}(0, d_S), \quad (16)$$

where $H_{c2}(0, d_S)$ is the field value obtained by linear extrapolation from the area $T \approx T_c$ into the area $T=0$. The parameter γ_M is determined from equation (15) after substitution of H_p into it.

Measurement of volt-ampere characteristic of tunnel *SNIN* and *NSIN* structures. The third method of measuring parameter γ_M is to measure the volt-ampere characteristics of *SNIN* and *NSIN* tunnel structures (*I* refers to an insulator). In [20, 21], state densities $N(\epsilon)$ at the interface between a compound electrode and insulator were calculated for various values of γ_M. At low temperatures $T \leq 0.1\ T_c$ the first derivative of the volt-ampere characteristic $dI/dV(V)$ coincides with the function $N(\epsilon)$. Figure 7*b* shows the function $N(\epsilon)$ at the interface between an *SN* electrode and insulator *I* of an *NSIN* structure for various values of d_S where $\gamma_M=0.5$. We can see that in *NSIN* structures it is also possible to determine the length of coherence in the *S* layer.

Thus, three methods have been suggested for determining parameter γ_M, allowing a study of the proximity effect at the boundary of various *S* and *N* metals and, based on these criteria, a search for the optimal parameters for the *NS-N-NS* variable-thickness microbridges before the junctions themselves are made.

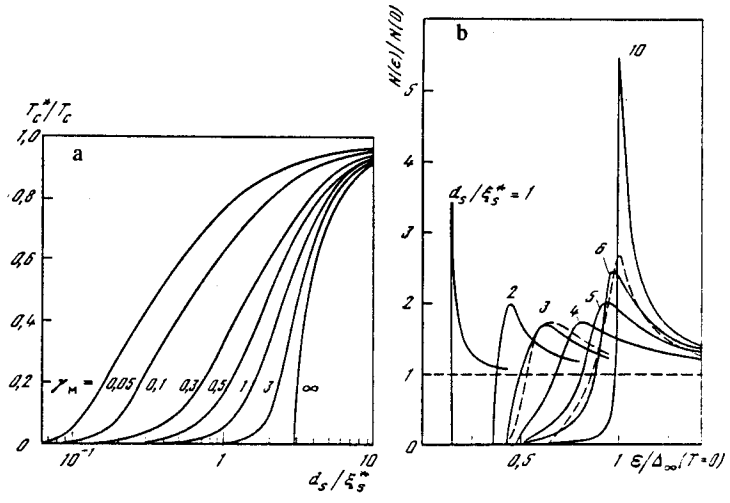

Figure 7. Critical Temperature of *SN* Sandwich as a Function of *S*-Layer Thickness for Various Values of γ_M (a) and State Density $N(\epsilon)$ at the Boundary of an *NS* Electrode and Insulator *I* in an *NSIN* Structure for γ_M=0.5 and Various Values of *S*-Layer Thickness where $T<T_c$. Dashed curves show experimental functions for Al-Al_2O_3-PbCd structures [19].

REFERENCES

1. Likharev, K. K., Yakobson, L. A. "Stationary Properties of Variable-Thickness Superconducting Bridges." ZhTF, 1973, Vol. 45, No. 7, pp. 1503-1509.

2. Kulik, I. O., Omelyanchuk, A. N. "The Microscopic Theory of the Josephson Effect in Superconducting Bridges." Pisma v ZhETF, 1975, Vol. 21, No. 4, pp. 216-219.

3. Likharev, K. K. "The $J_S(\varphi)$ Ratio for *SNS* Variable-Thickness Microbridges." Pisma v ZhTF, 1976, Vol. 2, No. 1, pp. 29-34.

4. Kodama, J., Hontsu, S., Hirai, H. "Stable Performance Nb Variable Thickness Microbridge Type Josephson Junctions: A Reproducible Fabrication Technique." J. Appl. Phys., 1983, Vol. 54, No. 6, pp. 3295-3301.

5. Ono, R. H., Sauvageau, J. E., Jain, A. K., et al. "Suspended Metal Mask Techniques in Josephson Junction Fabrication." J. Vac. Sci. and Technol., B., 1985, Vol. 3, No. 1, pp. 282-285.

6. De Lozanne, A. L., Anklam, W. J., Beasley, M. R. "Series Arrays of Refractory SNS Microbridges." Proc. Intern. Conf. Low Temp. Phys. LT-17, Karlsruhe, 1985, pp. 19-20.

7. Golubov, A. A., Kupriyanov, M. Yu., Lukichev, V. F. "Influence Of Proximity Effect and Electrodes on Stationary Properties of *SN-N-NS* Variable-Thickness Microbridges." Mikroelektronika, 1983, Vol. 12, No. 4, pp. 342-354.

8. Zaikin, A. D., Zharkov, G. F. "The Theory of 'Dirty' *SNS* Contacts." Fizika nizkikh temperatur, 1981, Vol. 7, No. 3, pp. 375-378.

9. Kupriyanov, M. Yu., Likharev, K. K., Lukichev, V. F. "Influence of Effective Interaction of Electrons on Critical Weak Coupling Josephson Current." ZhETF, 1982, Vol. 83, No. 7, pp. 431-441.

10. Lukichev, V. F. "Theoretical Study of Stationary Properties of Josephson Structures with Direct Conductivity." Dissertation for candidate of physical-mathematical sciences, 01.04.03, Moscow State University, 1982, 176 pp.

11. Kawakami, T., Takayanagi, H. "Single-Crystal *n*-InAs Coupled Josephson Junction." Appl. Phys. Lett., 1985, Vol. 46, No. 1, pp. 92-94.

12. Altukhov, A. A., Belevskiy, V. P., Valiyev, K. A., et al. "Structure, Composition and Superconducting Properties of Very Thin Films of Niobium Condensed Under Conditions of Autoion Bombardment." Mikroelektronika, 1985, Vol. 14, No. 1, pp. 45-49.

13. Baryshev, Yu. P., Valiyev, K. A., Mokrousov, K. Ya., et al. "Study of Dry Etching of Nb Films in CF_4/O_2 Plasma." Ibid, pp. 87-90.

14. Van Duzer, T., Turner, C. W. "Principles of Superconductive Devices and Circuits." Elsevier North Holland, Inc., 1981.

15. Kupriyanov, M. Yu., Lukichev, V. F., Orlikovskiy, A. A. "Stationary Properties of Quasi-Two-Dimensional Josephson Weak Couplings." Mikroeletronika, 1986, Vol. 15, No. 3, pp. 1244-1248.

16. Integralnye skhemy mikroelektroniki i ustroystva na sverkhprovodnikakh (Integrated Microelectronic Circuits and Superconducting Devices). Edited by V. N. Alfeyev, Moscow, Radio i svyaz Press, 1985, 232 pp.

17. Golubov, A. A., Kupriyanov, M. Yu., Lukichev, V. F., Orlikovskiy, A. A. "*SN*-Sandwich Critical Temperature." Mikroelektronika, 1983, Vol. 12, No. 4, pp. 355-362.

18. Kupriyanov, M. Yu. "The Second Critical Field in Two-Layer Systems." Fizika nizkikh temperatur, 1985, Vol. 11, No. 12, pp. 1244-1248.

19. Toplikar, J. R., Finnemore, D. K. "Electron-Tunneling Study of the Superconducting Proximity Effect in PbCd." Phys. Rev. B-Solid State, 1977, Vol. 16, No. 5, pp. 2072-2080.

20. Golubov, A. A., Kupriyanov, M. Yu., Lukichev, V. F. "Josephson Effect Theory in Tunnel *SNINS* and *SNIS* Structures." Fizika nizkikh temperatur, 1984, Vol. 10, No. 8, pp. 799-811.

21. Golubov, A. A., Kupriyanov, M. Yu. "Determining the Parameters of Superconducting Films in Tunnel *NSIN* Structures." Mikroelectronika, 1985, Vol. 14, No. 5, pp. 428-430.